Archive of Applied Mechanics 69 (1999) 257 - 264 © Springer-Verlag 1999

Numerical solution of singular integral equations in stress concentration problems under longitudinal shear loading

N. A. Noda, T. Matsuo

Summary The paper deals with numerical solutions of singular integral equations in stress concentration problems for longitudinal shear loading. The body force method is used to formulate the problem as a system of singular integral equations with Cauchy-type singularities, where unknown functions are densities of body forces distributed in the longitudinal direction of an infinite body. First, four kinds of fundamental density functions are introduced to satisfy completely the boundary conditions for an elliptical boundary in the range $0 \leq \phi_k \leq 2\pi$. To explain the idea of the fundamental densities, four kinds of equivalent auxiliary body force densities are defined in the range $0 \leq \phi_k \leq \pi/2$, and necessary conditions that the densities must satisfy are described. Then, four kinds of fundamental density functions are explained as sample functions to satisfy the necessary conditions. Next, the unknown functions of the body force densities are approximated by a linear combination of the fundamental density functions and weight functions, which are unknown. Calculations are carried out for several arrangements of elliptical holes. It is found that the present method yields rapidly converging numerical results. The body force densities and stress distributions along the boundaries are shown in figures to demonstrate the accuracy of the present solutions.

Key words elasticity, stress concentration, body force method, longitudinal shear, singular integral equation

1 Introduction

The body force method [1–3] has been applied to many important problems in the stress analysis. In the conventional body force method, the unknown functions of the body force densities are approximated by the products of the fundamental density functions and weight functions. Here, (a) the fundamental density function is an exact density of the body force to express a 2D solution for a single elliptical hole or crack; (b) the weight function is chosen to be a step function, which takes a constant value along each segment of the boundary discretization.

However, the following questions have not been settled yet:

(1) Why, in some cases, unknown body force densities do not converge with increasing numbers of collocation points?
(2) Why, in some cases, boundary conditions cannot be satisfied completely with increasing numbers of collocation points?
(3) How can we obtain smooth stress distributions along the boundary? Usually, that is very difficult to obtain because unknown functions are approximated by step functions.
(4) Tensile stress fields have been mainly treated as external loadings. Can other stress fields, such as in-plane shear, be analyzed with high accuracy?

Received 26 May 1998; accepted for publication 27 November 1998

N. A. Noda
Department of Mechanical Engineering,
Kyushu Institute of Technology,
Kitakyushu 804-8550, Japan

T. Matsuo
Department of Mechanical Engineering,
Fukushima National College of Technology,
Iwaki 970-8034, Japan

To answer these questions, numerical solutions of singular integral equations of the body force method are considered in this paper using as an example the longitudinal shear loading problems, where similar questions as in (1)–(3) also appear if we apply the conventional method.

The proposed new method [4–6] is applied to arbitrary distributed elliptical holes in an infinite body under longitudinal shear. The results show that the introduction of the new fundamental density functions can yield rapid converging numerical results and satisfy the boundary conditions along the entire boundary. It is also found that the method yields with high accuracy a smooth stress variation along the boundary.

2
Numerical solution for singular integral equations under longitudinal shear loading

2.1
Singular integral equations of the body force method

Consider several elliptical holes (the number of holes is m) in an infinite body under longitudinal shear τ_{zx}^{∞}, τ_{yz}^{∞} shown in Fig. 1. The problem can be formulated in terms of singular integral equations by using the stress field at an arbitrary point (x_i, y_i) when a point force acts on another point (ξ_k, η_k) in an infinite body. The formulation is simply based on the principle of superposition. The integral equation is expressed in the following Eq. (1), where the body force densities distributed along the prospective boundaries in the z-direction ($k = 1, \ldots, m$) are unknown functions:

$$-\frac{1}{2}\rho_z^*(\theta_i) + \sum_{k=1}^{m} \int_{\Gamma_k} K_{nz}^{Fz}(\phi_k, \theta_i)\rho_z^*(\phi_k)\, ds = -(\tau_{zx}^{\infty} \cos\theta'_{i0} + \tau_{yz}^{\infty} \sin\theta'_{i0}) \qquad (1)$$

$$i = 1 \sim m, \quad 0 \le \theta_i \le 2\pi \ .$$

Here, ϕ_k is the angle that specifies the points where body forces are distributed.

Equation (1) enforces the boundary conditions at the i-th elliptical boundary Γ_i; that is, $\tau_{nz}^{\infty} = 0$. Here, $\theta'_{i0} = \theta_{i0} + \psi_i$; θ_{i0} is the angle between the x-axis and the normal direction at the point (x_i, y_i) on the i-th ellipse, ψ_i is the angle between x_i-axis and x-axis. The function $K_{nz}^{Fz}(\phi_k, \theta_i)$ means the shear stress induced at the point when the body force with unit density in the z-direction is acting at the infinitesimal arc length on the k-th elliptical boundary Γ_k. Equation (1) has a Cauchy-type singularity in the case $i = k$. In the case $\theta_i = \phi_i$, the integration should be interpreted in the sense of Cauchy's principle values. The unknown functions in Eq. (1) $\rho_z^*(\phi_k)$ are expressed by the following equation:

$$\rho_z^*(\phi_k) = \frac{dF_z^*}{ds} \quad k = 1, \ldots, m \ . \qquad (2)$$

Here, dF_z^* is the resultant of the body force acting on the infinitesimal arc length ds.

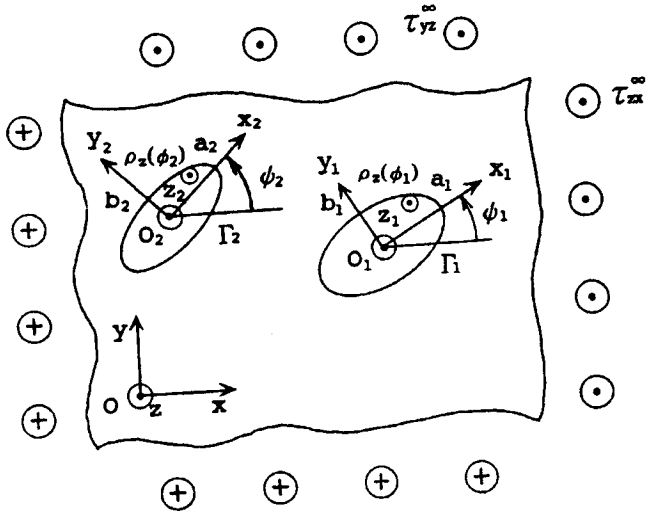

Fig. 1. Arbitrarily distributed elliptical holes under longitudinal shear loading

2.2
Fundamental density functions for the longitudinal shear problem

Here, auxiliary functions $\rho^*_{z1}(\phi_k) - \rho^*_{z4}(\phi_k)$ are defined in Eq. (3); these functions must satisfy Eqs. (4).

$$\begin{aligned}
\rho^*_{z1}(\phi_k) &= \tfrac{1}{4}[\rho^*_z(\phi_k) + \rho^*_z(\pi - \phi_k) + \rho^*_z(\pi + \phi_k) + \rho^*_z(-\phi_k)] \ , \\
\rho^*_{z2}(\phi_k) &= \tfrac{1}{4}[\rho^*_z(\phi_k) + \rho^*_z(\pi - \phi_k) - \rho^*_z(\pi + \phi_k) - \rho^*_z(-\phi_k)] \ , \\
\rho^*_{z3}(\phi_k) &= \tfrac{1}{4}[\rho^*_z(\phi_k) - \rho^*_z(\pi - \phi_k) - \rho^*_z(\pi + \phi_k) + \rho^*_z(-\phi_k)] \ , \\
\rho^*_{z4}(\phi_k) &= \tfrac{1}{4}[\rho^*_z(\phi_k) - \rho^*_z(\pi - \phi_k) + \rho^*_z(\pi + \phi_k) - \rho^*_z(-\phi_k)] \ ,
\end{aligned} \tag{3}$$

$$\begin{aligned}
\rho^*_{z1}(\phi_k) &= \rho^*_{z1}(\pi - \phi_k) = \rho^*_{z1}(\pi + \phi_k) = \rho^*_{z1}(-\phi_k) \ , \\
\rho^*_{z2}(\phi_k) &= \rho^*_{z2}(\pi - \phi_k) = -\rho^*_{z2}(\pi + \phi_k) = -\rho^*_{z2}(-\phi_k) \ , \\
\rho^*_{z3}(\phi_k) &= -\rho^*_{z3}(\pi - \phi_k) = -\rho^*_{z3}(\pi + \phi_k) = \rho^*_{z3}(-\phi_k) \ , \\
\rho^*_{z4}(\phi_k) &= -\rho^*_{z4}(\pi - \phi_k) = \rho^*_{z4}(\pi + \phi_k) = -\rho^*_{z4}(-\phi_k) \ .
\end{aligned} \tag{4}$$

It should be noted from Eqs. (4) that obtaining the functions $\rho^*_{z1}(\phi_k) - \rho^*_{z4}(\phi_k)$ in the region of $0 \le \phi_k \le \pi/2$ corresponds to obtaining the function $\rho^*_z(\phi_k)$ in the region of $0 \le \phi_k \le 2\pi$. In other words, if $\rho^*_{z1}(\phi_k) - \rho^*_{z4}(\phi_k)$ are given in the region of $0 \le \phi_k \le \pi/2$, $\rho^*_z(\phi_k)$ is given in the region of $0 \le \phi_k \le 2\pi$ as shown in Eqs. (5)

$$\begin{aligned}
\rho^*_z(\phi_k) &= \rho^*_{z1}(\phi_k) + \rho^*_{z2}(\phi_k) + \rho^*_{z3}(\phi_k) + \rho^*_{z4}(\phi_k) \ , \\
\rho^*_z(\pi - \phi_k) &= \rho^*_{z1}(\phi_k) + \rho^*_{z2}(\phi_k) - \rho^*_{z3}(\phi_k) - \rho^*_{z4}(\phi_k) \ , \\
\rho^*_z(\pi + \phi_k) &= \rho^*_{z1}(\phi_k) - \rho^*_{z2}(\phi_k) - \rho^*_{z3}(\phi_k) + \rho^*_{z4}(\phi_k) \ , \\
\rho^*_z(-\phi_k) &= \rho^*_{z1}(\phi_k) - \rho^*_{z2}(\phi_k) + \rho^*_{z3}(\phi_k) - \rho^*_{z4}(\phi_k) \ .
\end{aligned} \tag{5}$$

The fundamental density functions for longitudinal shear loading are defined by the following Eqs. (6); they are good examples of continuous auxiliary functions (3) because they satisfy Eqs. (4):

$$\begin{aligned}
w_{z1}(\phi_k) &= \frac{n_z(\phi_k)}{\cos\phi_k} \ , \\
w_{z2}(\phi_k) &= n_z(\phi_k) \quad \tan\phi_k \ , \\
w_{z3}(\phi_k) &= n_z(\phi_k) \ , \\
w_{z4}(\phi_k) &= n_z(\phi_k) \quad \sin\phi_k \ ,
\end{aligned} \tag{6}$$

Here, $n_z(\phi_k)$ is the x_k component of the normal unit vector at the point (x_k, y_k) on the prospective boundary, and is expressed by the following equation:

$$n_z(\phi_k) = \frac{b_k \cos\phi_k}{\sqrt{a_k^2 \sin^2\phi_k + b_k^2 \cos^2\phi_k}} = \cos\theta_{k0} \ . \tag{7}$$

The fundamental density functions defined by Eqs. (6) are shown in Fig. 2 for a circular boundary. Using these equations, $\rho^*_{z1}(\phi_k) - \rho^*_{z4}(\phi_k)$ are expressed in Eq. (8)

$$\begin{aligned}
\rho^*_{z1}(\phi_k) &= \rho_{z1}(\phi_k) w_{z1}(\phi_k) \ , \quad \rho^*_{z2}(\phi_k) = \rho_{z2}(\phi_k) w_{z2}(\phi_k) \ , \\
\rho^*_{z3}(\phi_k) &= \rho_{z3}(\phi_k) w_{z3}(\phi_k) \ , \quad \rho^*_{z4}(\phi_k) = \rho_{z4}(\phi_k) w_{z4}(\phi_k) \ ,
\end{aligned} \tag{8}$$

where

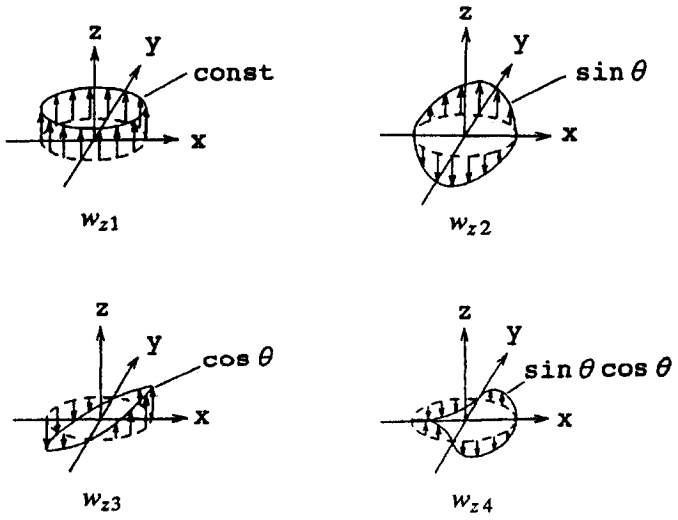

Fig. 2. Fundamental density functions for a circular boundary

$$f(\phi_k) = f(\pi - \phi_k) = f(\pi + \phi_k) = f(-\phi_k) \ . \tag{9}$$

The requirements that weight functions $\rho_{z1}(\phi_k) - \rho_{z4}(\phi_k)$ should satisfy are expressed in Eq. (9). Finally, the unknown function $\rho_z^*(\phi_k)$ is expressed as the sum of products of corresponding weight functions $\rho_{z1}(\phi_k) - \rho_{z4}(\phi_k)$ and $w_{z1}(\phi_k) - w_{z4}(\phi_k)$ shown in Eq. (10)

$$\rho_z^*(\phi_k) = \rho_{z1}(\phi_k)w_{z1}(\phi_k) + \rho_{z2}(\phi_k)w_{z2}(\phi_k) + \rho_{z3}(\phi_k)w_{z3}(\phi_k) + \rho_{z4}(\phi_k)w_{z4}(\phi_k) \ . \tag{10}$$

2.3
Numerical solution of singular integral equation

Using the expressions in Eq. (10), the singular integral equation (1) is reduced to the following Eq. (11):

$$\begin{aligned} &-\frac{1}{2}\left[\frac{\rho_{z1}(\theta_i)}{\cos\theta_i} + \rho_{z2}(\theta_i)\tan\theta_i + \rho_{z3}(\theta_i) + \rho_{z4}(\theta_i)\sin\theta_i\right]\cos\theta_{i0} \\ &\quad + \sum_{k=1}^{m}\int_0^{2\pi} K_{nz}^{Fz}(\phi_k,\theta_i)\left[\frac{\rho_{z1}(\phi_k)}{\cos\phi_k} + \rho_{z2}(\phi_k)\tan\phi_k + \rho_{z3}(\phi_k) + \rho_{z4}(\phi_k)\sin\phi_k\right] b_k\cos\phi_k \mathrm{d}\phi_k \\ &\quad = -(\tau_{zx}^{\infty}\cos\theta_{i0} + \tau_{yz}^{\infty}\sin\theta_{i0}) \quad i = 1 \sim m, \ \ 0 \le \theta_i \le 2\pi \ . \end{aligned} \tag{11}$$

In the present analysis, polynomials $t_n(\phi_k)$ have been used to approximate the unknown weight functions as continuous function,

$$\begin{aligned} \rho_{z1}(\phi_k) &= \sum_{n=1}^{M/4} a_n t_n(\phi_k), \quad \rho_{z2}(\phi_k) = \sum_{n=1}^{M/4} b_n t_n(\phi_k) \ , \\ \rho_{z3}(\phi_k) &= \sum_{n=1}^{M/4} c_n t_n(\phi_k), \quad \rho_{z4}(\phi_k) = \sum_{n=1}^{M/4} d_n t_n(\phi_k) \ , \end{aligned} \tag{12}$$

$$t_n(\phi_k) = \cos\{2(n-1)\phi_k\}, \tag{13}$$

where M is the number of the collocation points in the range of $0 \le \phi_k \le 2\pi$. Using the approximation method mentioned above, we obtain the following system of linear equation for the determination of the coefficients a_n, b_n, c_n, d_n where the number of unknown coefficients is Mm:

$$\sum_{k=1}^{m}\sum_{n=1}^{M/4}(a_nA_n + b_nB_n + c_nC_n + d_nD_n) = -(\tau_{zx}^{\infty}\cos\theta_{i0} + \tau_{yz}^{\infty}\sin\theta_{i0}) \qquad (14)$$

$$i = 1 \sim m, \quad 0 \le \theta_i \le 2\pi \ ,$$

with

$$\begin{aligned}
A_n &= -(1/2)t_n(\theta_i)\frac{\cos\theta_{i0}}{\cos\theta_i} + \int_0^{2\pi} K_{nz}^{Fz}(\phi_k,\theta_i)t_n(\phi_k)b_k\,\mathrm{d}\phi_k \ ,\\
B_n &= -(1/2)t_n(\theta_i)\cos\theta_{i0}\,\tan\theta_i + \int_0^{2\pi} K_{nz}^{Fz}(\phi_k,\theta_i)t_n(\phi_k)b_k\sin\phi_k\,\mathrm{d}\phi_k \ ,\\
C_n &= -(1/2)t_n(\theta_i)\cos\theta_{i0} + \int_0^{2\pi} K_{nz}^{Fz}(\phi_k,\theta_i)t_n(\phi_k)b_k\cos\phi_k\,\mathrm{d}\phi_k \ ,\\
D_n &= -(1/2)t_n(\theta_i)\cos\theta_{i0}\,\sin\theta_i + \int_0^{2\pi} K_{nz}^{Fz}(\phi_k,\theta_i)t_n(\phi_k)b_k\sin\phi_k\cos\phi_k\,\mathrm{d}\phi_k \ .
\end{aligned} \qquad (15)$$

The stresses at an arbitrary point are represented by a linear combination of the coefficients $a_n - d_n$ and the influence coefficients corresponding to $A_n - D_n$. Using the numerical solution mentioned above we will discuss interaction effects under longitudinal shear loading.

3
Numerical results and discussion

3.1
Interaction effect of two equal elliptical holes

An interaction problem of two equal elliptical holes in an infinite body under uniform z-direction shear stress τ_{zx}^{∞}, τ_{yz}^{∞} is shown in Fig. 3.

The stress τ_{tz} is calculated along the hole boundary when the central point of elliptical hole $i = 2$ is fixed at the origin, and the central point of elliptical hole $i = 1$ is moved from point A to E. Here, $a = 0.8$, $b = 0.9$, $\psi_1 = 0°$, $\tau_{zx}^{\infty} = 0$, $\tau_{yz}^{\infty} = 1$. Table 1 shows the convergence of the unknown functions ρ_{z1}, ρ_{z2}, ρ_{z3}, ρ_{z4} along the boundary with increasing the collocation number when the hole $i = 1$ is on B. Figure 4 shows the variation of the unknown weight functions ρ_{z1}, ρ_{z2}, ρ_{z3}, ρ_{z4}. In the present results, four unknown weight functions seem to approximate the real continuous density distributions very well because the present results for $M/4 = 8$ and $M/4 = 12$ coincide with each other to the fifth digits.

The distributions of the stress τ_{tz} along the boundary are shown in Fig. 5 when the central point of hole $i = 1$ is moved from point A to E and $\psi_1 = 0°$. In this figure, the results for a single hole are also shown by the dotted line. The maximum stress appears at $\theta = 0°$ and 180° when a single hole is subject to $\tau_{yz}^{\infty} = 1$. For two elliptical holes, it is found that the interaction effect is small near $\theta = 0°$. On the other hand, interaction effect is large near $\theta = 180°$.

The distributions of the stress τ_{tz} along the boundary of the hole $i = 1$ are shown in Fig. 6 when the inclination angle ψ_1 of the hole $i = 1$ is changed: $\psi_1 = 0°$, 30°, 60°, 90°. Here, $a = 0.8$,

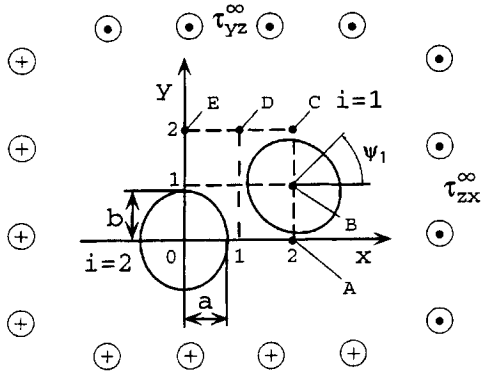

Fig. 3. Two equal elliptical holes under longitudinal shear loading $i = 1 : x = a\cos(\theta_1 + \psi_1) + x_1$, $y = b\sin(\theta_1 + \psi_1) + y_1$ $i = 2 : x = a\cos\theta_2$, $y = b\sin\theta_2$

Table 1. Body force densities along the boundary $i = 1$ (Fig. 3) for $\tau_{yz}^{\infty} = 1$, $a = 0.8$, $b = 0.9$, $\psi_1 = 0°$

θ_1 (deg.)	M/4	ρ_{z1}	ρ_{z2}	ρ_{z3}	ρ_{z4}
0	4	0.2682	1.6962	−0.3730	0.0361
	8	0.2659	1.6948	−0.3707	0.0364
	12	0.2659	1.6948	−0.3707	0.0364
20	4	0.1634	1.7827	−0.2868	−0.0518
	8	0.1652	1.7843	−0.2886	−0.0524
	12	0.1652	1.7843	−0.2886	−0.0524
40	4	−0.0231	1.8877	−0.1143	−0.1815
	8	−0.0239	1.8863	−0.1133	−0.1809
	12	−0.0239	1.8863	−0.1133	−0.1809
60	4	−0.1259	1.8828	0.0091	−0.2207
	8	−0.1256	1.8836	0.0087	−0.2212
	12	−0.1256	1.8836	0.0087	−0.2212
80	4	−0.1486	1.8569	0.0527	−0.2188
	8	−0.1486	1.8566	0.0528	−0.2186
	12	−0.1486	1.8566	0.0528	−0.2186
90	4	−0.1497	1.8540	0.0566	−0.2183
	8	−0.1500	1.8523	0.0572	−0.2173
	12	−0.1500	1.8523	0.0572	−0.2173

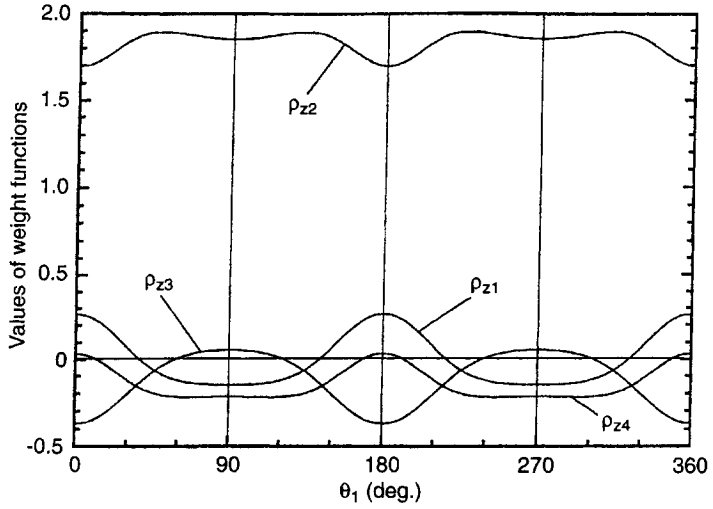

Fig. 4. Weight functions of the present analysis in Fig. 3 for $\tau_{yz}^{\infty} = 1$, $a = 0.8$, $b = 0.9$, $\psi_1 = 0°$

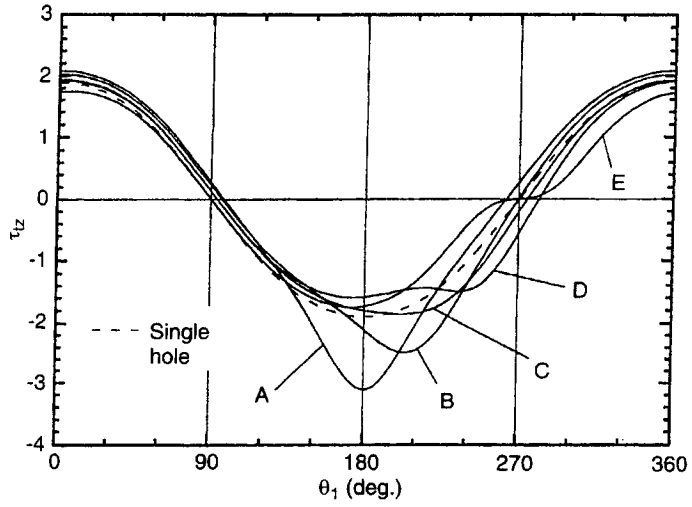

Fig. 5. Stress distribution along the boundary $i = 1$ in Fig. 3 for $\tau_{yz}^{\infty} = 1$, $a = 0.8$, $b = 0.9$, $\psi_1 = 0°$

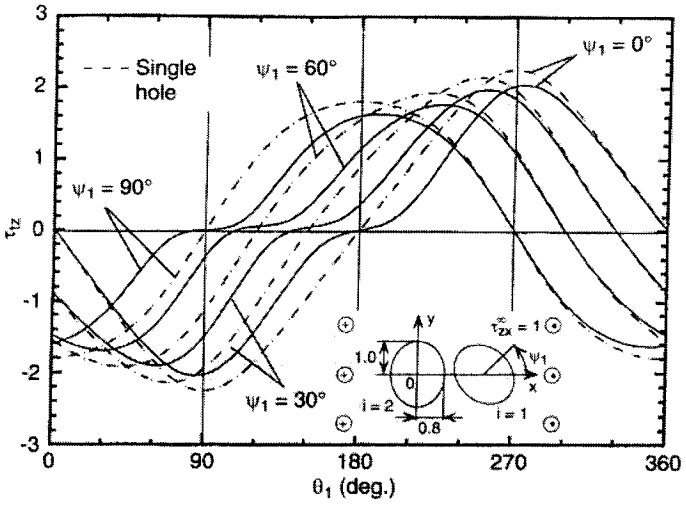

Fig. 6. Stress distribution along the boundary $i = 1$ in Fig. 3 for $\tau_{zx}^{\infty} = 1$, $a = 0.8$, $b = 0.9$

$b = 1.0$, $x_1 = 2.0$, $y_1 = 0.0$, $\tau_{zx}^{\infty} = 1$, $\tau_{yz}^{\infty} = 0$. It is found that the interaction effect is at the largest when the two inclusions are closest to each other.

3.2
Interaction effect of two different elliptical holes

Figure 7 shows two elliptical holes under longitudinal shear loading. Here, the interaction effects are calculated for different half-axes and different aspect ratios. The distributions of the stress τ_{tz} along the boundary of the hole $i = 1$ are shown in Fig. 8 for $a_1 = 0.8$, $b_1 = 0.9$,

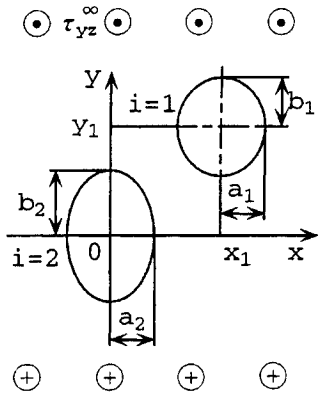

Fig. 7. Two different elliptical holes under longitudinal shear loading
$i = 1$: $x = a_1 \cos\theta_1 + x_1$, $y = b_1 \sin\theta_1 + y_1$
$i = 2$: $x = a_2 \cos\theta_2$, $y = b_2 \sin\theta_2$

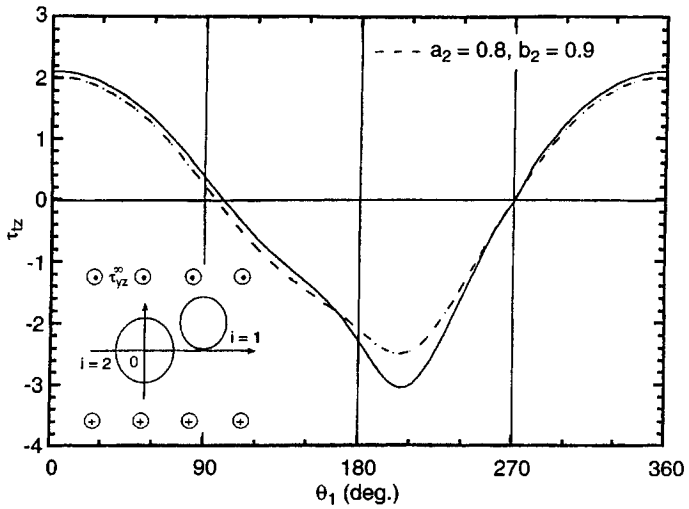

Fig. 8. Stress distribution along the boundary $i = 1$ in Fig. 7 for $a_1 = 0.8$, $b_1 = 0.9$, $x_1 = 2.0$, $y_1 = 1.0$, $a_2 = 1.0$, $b_2 = 1.125$

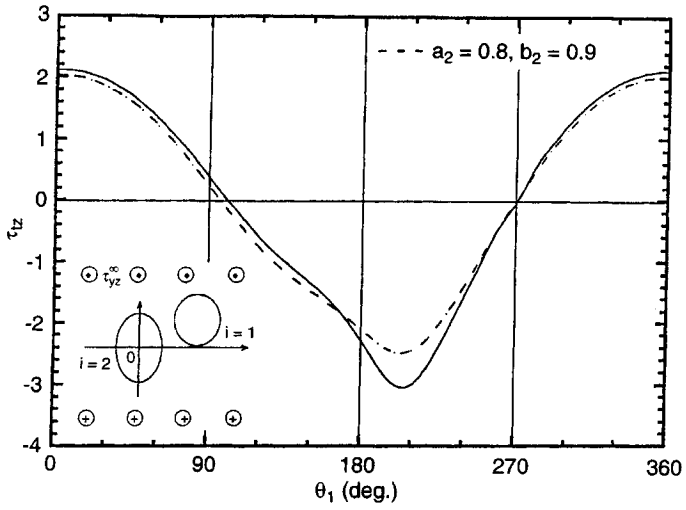

Fig. 9. Stress distribution along the boundary $i = 1$ in Fig. 7 for $a_1 = 0.8$, $b_1 = 0.9$, $x_1 = 2.0$, $y_1 = 1.0$, $a_2 = 0.8$, $b_2 = 1.2$

$x_1 = 2.0$, $y_1 = 1.0$, $a_2 = 1.0$, $b_2 = 1.125$. The distributions of the stress τ_{tz} along the boundary of the hole $i = 1$ are shown in Fig. 9 for $a_1 = 0.8$, $b_1 = 0.9$, $x_1 = 2.0$, $y_1 = 1.0$, $a_2 = 0.8$, $b_2 = 1.2$. In these figures, the results for $a_2 = 0.8$, $b_2 = 0.9$ (i.e. for equal two elliptical holes) are also shown by the dotted line. It is found that the interaction effect is larger at nearly 180°.

4
Conclusions

In this paper, the interaction problem of arbitrarily distributed elliptical holes under longitudinal shear loading has been discussed as an example of a numerical solution to singular integral equations of the body force method. The problem has been formulated in terms of singular integral equations with the Cauchy-type singularity. Within the body force method the Green's functions for a point force have been used as fundamental solutions. In the analysis, the unknown functions of the body force densities have been approximated by a linear combination of the fundamental density functions and weight functions. To satisfy the boundary condition along the boundary under longitudinal shear loading, four kinds of fundamental density functions of the body force have been proposed. It has been found that the boundary conditions were satisfied with high degree of accuracy, and smooth stress distributions could be calculated along the boundary. The present method has been applied to several problems. It has been found that the method is effective for numerical analyses regarding different half-axes, different aspect ratios, inclinations and locations.

References

1. **Nisitani, H.:** The two-dimensional stress problem solved using an electric digital computer. J. Japan Soc. Mech. Eng. 70 (1967) 627–632
2. **H. Nisitani, H.:** Solution of notch problems by body force method. In: G.H. Sih (ed.) Stress analysis of notched problem 1–68, Noordhoff International Publication: Leiden (1974)
3. **Nisitani, H.; Chen, D. H.:** The body force method (Taisekiryokuho in Japanese). Baifukan Publication: Tokyo (1987)
4. **Noda, N. A.; Matsuo, T.:** Singular integral equation method in the analysis of interaction between crack and defects. Fracture Mech. (25) 1220, American Society for Testing and Materials, (1995) 591–605
5. **Noda, N. A.; Matsuo, T.:** Numerical solution of singular integral equations in stress concentration problems. Int. J. Solids Struct. 34-19 (1997) 2429–2444
6. **Noda, N. A.; Matsuo, T.:** Singular integral equation method for interaction between elliptical inclusions. Trans. ASME J. Appl. Mech. 65 (1998) 310–319